Control and Locomotion of Hydrodynamically Coupled Rigid Spheres

Tony Dear¹, Scott David Kelly², and Howie Choset¹

Abstract—The coupling interactions between two spherical swimmers in an ideal fluid have known analytic approximations for certain types of motion. We apply these results to produce locomotion and coordination through the actuation of internal masses inside each swimmer. Through control of either both swimmers or one of them, the latter case taking advantage of compliance in the passive swimmer, desired motion along the spheres' line of centers can be achieved. We subsequently treat general 2D motion as a superposition of motion components along and perpendicular to the spheres' line of centers, leading to a derivation of a full model of controlled locomotion and coordination of two spheres in a planar fluid.

I. INTRODUCTION

The swimming locomotion of deformable or rigid bodies is often difficult to model analytically due to the complexity of the governing hydrodynamics. For solitary bodies, motion may be achieved through temporal deformation of the body's shape. This "self-propulsion" has been described for various geometries in both ideal fluids [1]–[3] and viscous incompressible fluids [4]–[6]. Many of these results approximate locomotion as a result of momentum conservation between the body and the surrounding fluid, allowing for a generic derivation of controllability [7]. If a body is unable to deform its shape, then motion due to momentum exchange can also occur by varying its internal mass geometry [8].

Alternatively, submerged rigid bodies can be induced to move due to external interactions with the surrounding fluid or with other bodies nearby. Lamb [9] and Milne-Thomson [10] provide approximations for the interactions between two spheres in an ideal fluid when motion is induced either along or perpendicular to their line of centers. Nair and Kanso [11] build upon these analyses to explore the coupling between generic rigid bodies along a common axis, including motion coordination between a fixed and a free body.

In this work we combine various aspects of the cited works to develop a general planar model for *actuated* locomotion of two rigid spheres in an ideal fluid. Like the analysis of Kozlov and Onishchenko [8], the spheres move in response to variation in internal mass distribution. We use the results of Lamb [9] and Milne-Thomson [10] to derive an approximate, analytic form of a multi-body Lagrangian. Unlike Nair and Kanso [11], we can accommodate free bodies as well as motion that is not along a common axis. We mainly consider *periodic* actuation of these bodies, wherein movement of the

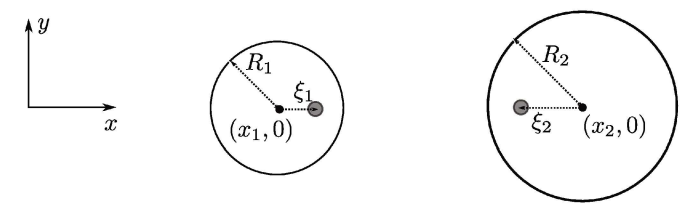


Fig. 1: Two spherical swimmers, each with an internal mass. The swimmers can move along the inertial x axis, with positions given by x_1 and x_2 , as can the internal masses, with positions ξ_1 and ξ_2 from the respective sphere centers.

bodies' internal masses is constrained by linear springs. This feature allows us to study aspects of submerged mass-spring systems, such as passive locomotion [12] and synchronization [13], [14], in the context of coupled rigid bodies.

The organization of the rest of this paper is as follows. The following section will review the solution of spheres oscillating along the line of centers and introduce the actuation mechanism of using controlled internal masses in each sphere. We use transfer function analysis to show that only one input is actually necessary for both spheres to move in a desired way, with the passive sphere simply reacting to an external propulsion. The next section then summarizes an analogous derivation for perpendicular oscillations, followed by a derivation of the full planar locomotion model as a superposition of the previous two.

II. SPHERICAL SWIMMERS MOVING ON A LINE

A. Hollow Spheres Model

The locomotion of two spheres moving either toward or away from each other along their line of centers can be described using the Lagrangian method. The derivation is done in detail by Lamb [9] and Milne-Thomson [10]; here, we briefly summarize the key points and explicitly show the order of the Lagrangian used in derivations in the rest of the paper. We first deal with the spheres without internal masses, as the latter contributions can be added later on.

As shown in Fig. 1, the positions of the spheres with respect to an inertial frame are given by $(x_1,0)$ and $(x_2,0)$, their radii are R_1 and R_2 , and their masses m_1 and m_2 . The surrounding fluid has density ρ . We consider the velocity potential ϕ_1 of the fluid, which must everywhere satisfy Laplace's equation, $\nabla^2\phi_1=0$. The boundary conditions are that the fluid is at rest infinitely far away from the spheres, while the motion of the spheres leads to a flux condition on

 $^{^1}$ T. Dear and H. Choset are with the Robotics Institute at Carnegie Mellon University, Pittsburgh, PA 15213, USA. {tonydear@, choset@cs.}cmu.edu

²S. D. Kelly is with the Department of Mechanical Engineering and Engineering Science at the University of North Carolina at Charlotte, Charlotte, NC 28223, USA. scott@kellyfish.net

the bodies' surfaces. The latter takes the form

$$-\frac{\partial}{\partial n}\phi_1(x,y) = \frac{x - x_i}{\sqrt{(x - x_i)^2 + y^2}} \dot{x}_i, \quad i = 1, 2,$$
 (1)

where $-\frac{\partial \phi_1}{\partial n}$ is the flux going into each of the sphere surfaces. The coefficient in front of \dot{x}_i is such that the flux is greatest along the line of the spheres' motion and zero where the spherical surface tangent is parallel to it.

A solution can be obtained for ϕ_1 in the form of an infinite series using the method of image doublets [9], [10]. The kinetic energy of the fluid is then given by the integration

$$T_x = -\frac{1}{2}\rho \int \phi_1 \frac{\partial \phi_1}{\partial n} dS_1 - \frac{1}{2}\rho \int \phi_1 \frac{\partial \phi_1}{\partial n} dS_2$$
 (2)

over the surfaces of each sphere, denoted by S_1 and S_2 . The idea here is that $-\frac{\partial \phi_1}{\partial n}$ is the normal fluid velocity into each sphere, and $\rho\phi_1$ is an impulse that generates the motion. Integrating their product over both of the sphere surfaces then gives us the total kinetic energy from their motion.

As previously mentioned, the full form of ϕ_1 is that of an infinite series whose higher-order terms can be effectively ignored, since the two spheres cannot approach arbitrarily close to each other due to their finite radii. An analytical form for the kinetic energy can be written as

$$T_x(x_2 - x_1, \dot{x}_1, \dot{x}_2) = \frac{1}{2} M_1 \dot{x}_1^2 - N_x \dot{x}_1 \dot{x}_2 + \frac{1}{2} M_2 \dot{x}_2^2, \quad (3)$$

where M_i are the *effective masses* of each swimmer and N is a cross-coupling term between the two. Written up to order $(x_2 - x_1)^{-6}$, they are

$$\begin{split} M_i &= m_i + \frac{2}{3}\pi\rho R_i^3 \left(1 + \frac{3R_1^3R_2^3}{(x_2 - x_1)^6}\right), \quad i = 1, 2; \\ N_x &= 2\pi\rho \frac{R_1^3R_2^3}{|x_2 - x_1|^3}. \end{split}$$

For the simulations that we perform, higher-order terms are negligible even when the spheres are adjacent to each other. The relative contributions of these terms can be computed for different model parameters, but this truncation is generally sufficient when the two spheres are of similar size.

By deriving the Euler-Lagrange equations from Eq. (3), one can find the forces acting on each swimmer due to the motion of both. In particular, Lamb [9] notes the result of each sphere making small oscillations about their initial position along their line of centers. Assuming the same frequency for \dot{x}_1 and \dot{x}_2 , the mean value of the second-order terms in the Lagrange equations will be 0, and the average forces acting on the spheres are opposite with magnitude

$$F_x(x_2 - x_1, \dot{x}_1, \dot{x}_2) = 6\pi \rho \frac{R_1^3 R_2^3}{(x_2 - x_1)^4} [\dot{x}_1 \dot{x}_2], \qquad (4)$$

where $[\dot{x}_1\dot{x}_2]$ is the mean value of $\dot{x}_1\dot{x}_2$. If the phase offset between the two velocities is less than a quarter period, then $[\dot{x}_1\dot{x}_2]$ is positive and the spheres experience repulsion from each another; otherwise, the spheres experience an attractive force toward each other. Although the magnitude of F_x varies inversely with the spheres' distances from each other, we need not worry about F_x becoming unbounded since we assume finite, rigid radii for both spheres.

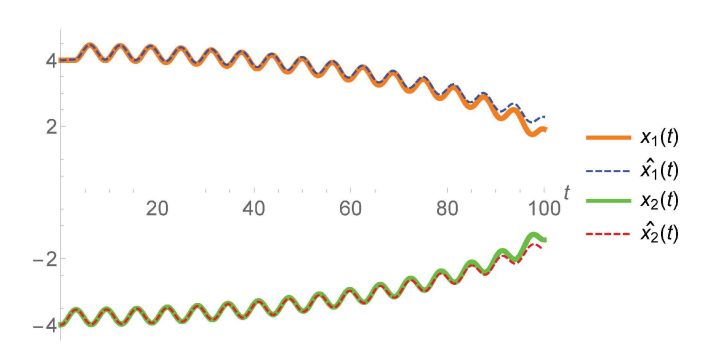


Fig. 2: The attraction of two spheres in response to out-of-phase perturbations of their internal masses. Solid trajectories $x_i(t)$ are computed via the full equations of motion; the dashed $\hat{x}_i(t)$ are a sum of individual and coupled approximations.

B. Adding Internal Masses

We now consider the presence of a small mass inside each sphere, each of which can move along the line of centers as an actuation mechanism for the spheres. Each sphere will also move along this axis as a result. If the masses inside swimmer 1 and swimmer 2 are μ_1 and μ_2 , respectively, and their configurations measured from their respective sphere centers are ξ_1 and ξ_2 , then their kinetic energy is

$$T_{\xi}(\dot{x}_{1},\dot{x}_{2},\dot{\xi}_{1},\dot{\xi}_{2}) = \frac{1}{2}\mu_{1}(\dot{x}_{1}+\dot{\xi}_{1})^{2} + \frac{1}{2}\mu_{2}(\dot{x}_{2}+\dot{\xi}_{2})^{2}. \tag{5}$$

The total kinetic energy of the system is then T_x+T_ξ , and by going through the derivation of the Euler-Lagrange equations as before, we can obtain the updated equations of motion and description of forces on the spheres. In particular, exciting ξ_1 and ξ_2 with periodic oscillations ensures that the force contributions from T_ξ have a mean value of 0, so Eq. (4) acting on the spheres remains unchanged.

If we assume that we have direct control over ξ_1 and ξ_2 , then this problem can be recast into a principal fiber bundle formulation [15], [16]. Specifically, we have a base space $B = \mathbb{R}^2$ formed by all possible mass configurations (ξ_1, ξ_2) and a set of fibers \mathbb{R}^2 defined by the positions (x_1, x_2) over B. In typical locomotion problems, the fibers form a symmetry group, allowing for reduction of the equations of motion to a simple mapping between the base and fiber velocities via a local connection form. In this problem, the fibers do not exhibit a group symmetry, since the spheres' effective masses depend on their relative displacement.

In cases in which the spheres are sufficiently far away from each other, the following approximation of a principal connection can be made. Momentum conservation dictates the response of each sphere due to actuation of its own internal mass, ignoring the presence of the other sphere. This gives us a constant, diagonal *mechanical connection* relating the mass velocities to the sphere's perturbation velocities as

$$\begin{bmatrix} \dot{x}_{1,p} \\ \dot{x}_{2,p} \end{bmatrix} = - \begin{bmatrix} \frac{\mu_1}{\mu_1 + M_1} & 0 \\ 0 & \frac{\mu_2}{\mu_2 + M_2} \end{bmatrix} \begin{bmatrix} \dot{\xi}_1 \\ \dot{\xi}_2 \end{bmatrix}. \tag{6}$$

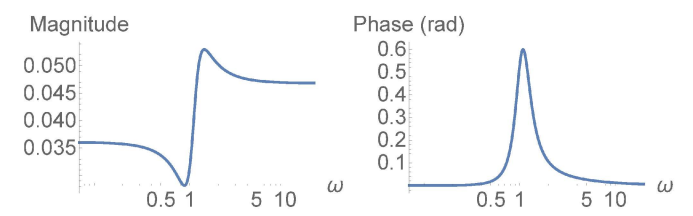


Fig. 3: Transfer function response from \dot{x}_1 to \dot{x}_2 as a function of input frequency of ξ_1 . The resonant frequency of the mass ξ_2 is 1 rad/s, close to the frequency of peak phase offset.

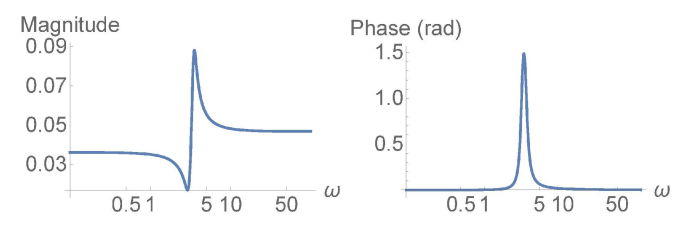


Fig. 4: Same as the previous figure, except with resonant frequency 3 rad/s. As a result, both the magnitude and phase response maxima are scaled up and shifted rightward.

A separate coupled response of the spheres' slow motion can then be computed by finding $[\dot{x}_1\dot{x}_2]=[\dot{x}_{1,p}\dot{x}_{2,p}]$ and integrating Eq. (4). The sum of the two responses, one kinematic and one dynamic, approximates that generated by the full equations of motion derived from Eq. (5). An example simulation showing the validity of this approximation is shown in Fig. 2. We set the parameters $\rho=1$, $R_1=R_2=2$, $m_1=m_2=0$, $\mu_1=\mu_2=5$, and command the inputs $\xi_1=\cos t$, $\xi_2=\cos(t-\frac{11\pi}{12})$.

Our first observation is that because the spheres' oscillations are nearly a half-cycle out of phase with each other, the forces on each are attractive, verifying Lamb's assertion [9]. Furthermore, the trajectories $\hat{x_i}(t)$ obtained from superimposing the individual and coupled responses of the spheres follow very closely the actual trajectories $x_i(t)$ from the full equations of motion. They only begin to diverge around t=90 as the spheres nearly collide. On the other hand, if the spheres were actuated so as to repel each other, this approximation would hold throughout.

C. A Compliant Spring-Loaded Mass

Rather than having control of both spheres, a more challenging example may be that we can only directly control one of the masses, while the other sphere moves according to the known hydrodynamics. Suppose that we can control the movement of the mass μ_1 , while μ_2 can oscillate freely due to attachment to the center of its sphere via a spring. This introduces a potential energy $V_{\xi} = \frac{1}{2}k_{\xi}\xi_2^2$, where k_{ξ} is the spring constant. The full system is now described by the Lagrangian

$$L_{x,\xi} = T_x + T_{\xi} - V_{\xi}. \tag{7}$$

The role of the spring in the sphere with the compliant mass, here assumed to be μ_2 , is to allow μ_2 to continue oscillating with no direct active input.

To produce any form of desired locomotion, a primary goal is to be able to produce either attraction or repulsion of the spheres while only commanding ξ_1 . To do this, it is useful to analyze the transfer function of the sphere velocities as a function of the input's frequency. We linearize the Euler-Lagrange equations derived from $L_{x,\xi}$ in Eq. (7) and obtain the matrices A and B in

$$\dot{X} = AX + B\xi_1,$$

where $X=(x_1,x_2,\xi_2,\dot{x}_1,\dot{x}_2,\dot{\xi}_2)$ comprise the states and ξ_1 is our input. The transfer function from \dot{x}_1 to \dot{x}_2 can then be derived as a function of the frequency of ξ_1 .

Figs. 3 and 4 show two instances of Bode response plots of this transfer function, both using the same parameters from the simulation of Fig. 2. Fig. 3 is the response with spring constant k=5 N/m; Fig. 4 has spring constant k=45 N/m. The magnitude plots for each show varying but finite levels of attenuation between the amplitudes of \dot{x}_1 and \dot{x}_2 , which is sensible since we only actuate ξ_1 directly.

The transfer function is biquadratic second-order in the form

$$H(s) = \frac{N_2 s^2 + N_1 s + N_0}{D_2 s^2 + D_1 s + D_0}$$

with all constants being positive, so the phase offset between \dot{x}_1 and \dot{x}_2 is close to 0 at both low and high input frequencies. This means that for most inputs, repulsion of the swimmers is the only result. However, close to the resonant frequency of the compliant mass $\omega_\xi = \sqrt{k_\xi/\mu_2}$, the phase offset can become much greater than 0, allowing for attractive behavior.

The optimal input frequency can be found numerically or analytically in terms of maximizing the phase or magnitude response, and choosing one is mainly a design decision that will impact the speed at which the swimmers are attracted or repelled. This analysis will appear in future work. Here we make a qualitative observation about how the phase response changes with respect to ω_{ξ} . For small values of ω_{ξ} , such as that of Fig. 3, the maximal phase may not be able to surpass $\frac{\pi}{4}$, so that it is impossible to produce attraction while only commanding ξ_1 . At the limit of $\omega_{\xi}=0$, μ_2 is disconnected from its encompassing sphere, leaving the latter with no mechanism to oscillate on its own.

For larger values of ω_ξ , the peak phase also becomes larger, allowing for a greater range of inputs that can produce attraction. However, a practical limitation is that a physical actuator is bounded in how fast it can operate. As $\omega_\xi \to \infty$, μ_2 essentially becomes rigidly attached to its sphere, again removing the oscillatory mechanism.

Finally, this analysis can be combined with that of the previous subsection to produce desired attractive or repulsive forces on the spheres. The input of ξ_1 produces a known oscillatory response in $\dot{x}_{1,p}$ through Eq. (6). We can obtain the corresponding response of $\dot{x}_{2,p}$ through the preceding transfer function analysis. The resultant forces on each sphere can then be computed via Eq. (4), which can subsequently be integrated to find the full system trajectories.

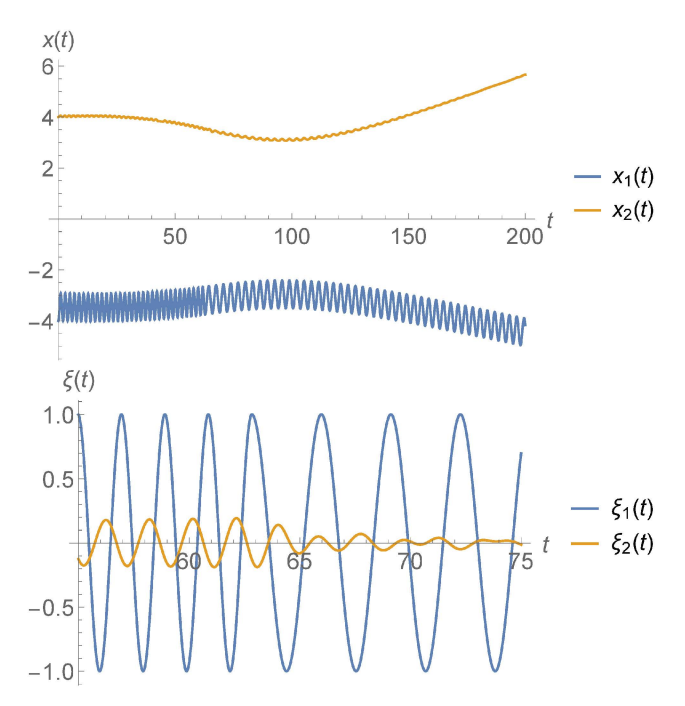


Fig. 5: Input frequencies to ξ_1 are chosen in order to produce attractive followed by repulsive locomotion of the spheres. The second plot shows a plot of ξ_1 around the transition time as well as the response of the compliant mass ξ_2 .

An example simulation is shown in Fig. 5. Here we use the parameters of the system used to derive the transfer function in Fig. 4, except with $\mu_1=20$ to make x_1 oscillate faster. Suppose we want the spheres to be first attracted toward and then later repelled from each other. We thus perturb μ_1 with two different frequency inputs, the first stage at 3.2 rad/s, and the second at 2 rad/s. In the first half, \dot{x}_1 and \dot{x}_2 are a quarter cycle out of phase; in the second, they are nearly completely in phase. As expected, the spheres are first attracted and then repelled, the latter occurring following a frequency, and thus phase, change in the input.

III. SPHERICAL SWIMMERS IN THE PLANE

A. Actuation Perpendicular to the Line of Centers

In order to motivate the planar locomotion problem of two coupled swimmers, we once again consider two hollow spheres, each now only oscillating along the axis perpendicular to their line of centers. Thus, using the inertial configuration of Fig. 6, the positions of the spheres are given by (x_1,y_1) and (x_2,y_2) . In this problem, the velocity potential ϕ_2 is subject to the boundary conditions

$$-\frac{\partial \phi_2}{\partial n} = \frac{y}{\sqrt{(x-x_i)^2 + y^2}} \dot{y}_i, \quad i = 1, 2, \tag{8}$$

on the sphere surfaces.

An approximate analytical solution can then be obtained for ϕ_2 and subsequently for the kinetic energy T_y , in a manner similar to that in the preceding section. This is

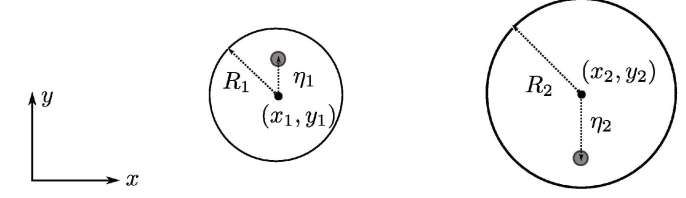


Fig. 6: Two spherical swimmers, each with an internal mass. Each of the latter can move in the inertial y direction, described by configurations η_1 and η_2 with respect to the sphere centers.

provided by Lamb [9] as

$$T_y(x_2 - x_1, \dot{y}_1, \dot{y}_2) = \frac{1}{2} M_1 \dot{y}_1^2 + N_y \dot{y}_1 \dot{y}_2 + \frac{1}{2} M_2 \dot{y}_2^2, \quad (9)$$

where M_1 and M_2 are the same as in T_x (Eq. 3) and $N_y = \frac{N_x}{2}$. Unlike T_x , the kinetic energy in this case has dependencies on all four configuration variables or their velocities, allowing for planar movement. Because we are ignoring \dot{x}_1 and \dot{x}_2 contributions to the Lagrangian here, this model is only valid as long as these velocities are sufficiently small; we consider the full model in the next subsection.

If we derive the Euler-Lagrange equations from T_y and assume that each sphere makes small oscillations in the y direction, we find that there is a equal and opposite average force on the spheres in the x direction with magnitude

$$F_y(x_2 - x_1, \dot{y}_1, \dot{y}_2) = 3\pi \rho \frac{R_1^3 R_2^3}{(x_2 - x_1)^4} [\dot{y}_1 \dot{y}_2]. \tag{10}$$

The direction that F_y acts on each of the spheres is opposite to that of F_x . The spheres thus experience attraction when \dot{y}_1 and \dot{y}_2 are in phase by at least a quarter cycle and repulsion otherwise. On the other hand, the average forces acting on the spheres in the y direction are 0, ensuring that the line of centers does not have net displacement or rotation over time. The present model assumes that the line of centers does not move at all, which is approximately true for small perturbations relative to the inter-sphere distance. However, this assumption will also be dropped in the next subsection for a more complete model.

For the actuation mechanism, we again assume the presence of an internal mass inside each sphere with configurations η_1 and η_2 , each allowed to move in the y direction. Note that the local mechanical connection relating the mass velocities to \dot{y}_1 and \dot{y}_2 is the same as in Eq. (6), due to spherical symmetry. If we can command η_1 directly and allow η_2 to be passively attached to a spring, then a transfer function analysis analogous to that in the previous section gives a range of input frequencies that lead to either attractive or repulsive locomotion.

Fig. 7 shows a Bode plot of the transfer function of \dot{y}_2 in response to \dot{y}_1 for the parameters $\mu_1=\mu_2=20,\ k=30,$ and the rest as previously assigned. Note that we use much heavier masses and a stiffer spring in order to obtain an appreciable magnitude response, as it is more difficult to make the passive mass move when perturbation is in the

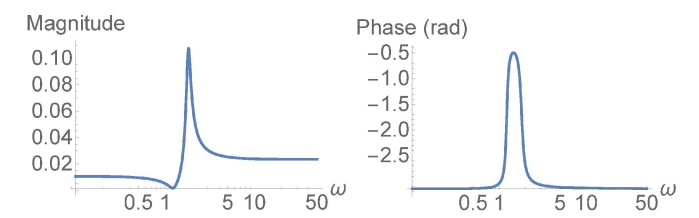


Fig. 7: Transfer function response from \dot{y}_1 to \dot{y}_2 as a function of input frequency of η_1 . For most frequencies, the two spheres move completely out of phase, leading to repulsion in the x direction.



Fig. 8: Sphere trajectories starting from initial positions (-4,0) and (4,0). Small oscillations of sphere 1 produce a small in-phase response in sphere 2, leading to attraction of the spheres along the x axis.

orthogonal direction. In contrast to Figs. 3 and 4, the default behavior is for the spheres to oscillate out of phase in the y direction, resulting in repulsion in the x direction. Close to the resonant frequency $\omega_{\eta} = \sqrt{k_{\eta}/\mu_{2}}$, there is again a range of input frequencies that will possibly result in the spheres moving in phase and being attracted to each other.

A parametric plot of the two spheres starting 8 units apart and subsequently moving toward each other is shown in Fig. 8. We perturb η_1 with a frequency of 1.5 rad/s, resulting in a phase difference of about -0.5 radians. Although the resultant magnitude of \dot{y}_2 is very small, the phase offset is sufficiently small enough to generate attraction in the x direction over time, even though both spheres are only oscillating in y.

B. General Planar Actuation

For general two-dimensional motion of the spheres, the velocity potential satisfies both boundary conditions (1) and (8) on the surfaces of each sphere and ends up as the superposition $\phi=\phi_1+\phi_2$ due to linearity of Laplace's equation. On the other hand, the resultant kinetic energy is not exactly the sum T_x+T_y , as this does not account for energy contributions from the cross terms, such as the y velocity of sphere 2 associated with an impulse of sphere 1 in the x direction and vice versa. One can verify from ϕ given in Milne-Thomson [10] that they are at least an order of magnitude smaller than N_x and N_y , the cross terms due to both spheres moving along the same direction. We thus posit that T_x+T_y is a reasonable approximation for the total energy of the system.

With the spheres now possibly accumulating nontrivial displacement in both inertial planar directions, we do not assume that the line of centers remains constant. The Lagrangian is thus defined with respect to a frame in which

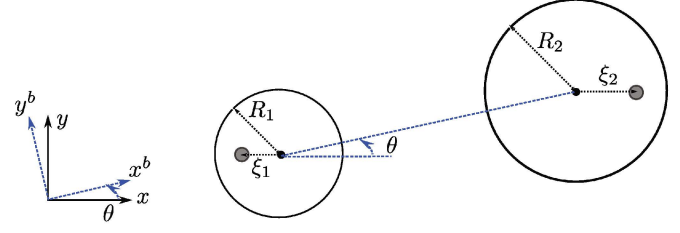


Fig. 9: Two spherical swimmers whose line of centers is aligned with a "body frame" $\{x^b, y^b\}$ that has an orientation θ with respect to the inertial frame. Each sphere has an internal mass whose configuration is aligned with the inertial x axis and can be directly actuated.

the coordinate axes rotate with the line of centers as the spheres move. From Fig. 9, we have that

$$x_2^b - x_1^b = \sqrt{(x_2 - x_1)^2 + (y_2 - y_1)^2},$$

$$\begin{bmatrix} \dot{x}_i^b \\ \dot{y}_i^b \end{bmatrix} = \begin{bmatrix} \cos \theta & \sin \theta \\ -\sin \theta & \cos \theta \end{bmatrix} \begin{bmatrix} \dot{x}_i \\ \dot{y}_i \end{bmatrix},$$
(11)

where

$$\tan \theta = \frac{y_2 - y_1}{x_2 - x_1}.$$

The total kinetic energy of two spheres undergoing planar motion is thus given by

$$T^{b} = T_{x}(x_{2}^{b} - x_{1}^{b}, \dot{x}_{1}^{b}, \dot{x}_{2}^{b}) + T_{y}(x_{2}^{b} - x_{1}^{b}, \dot{y}_{1}^{b}, \dot{y}_{2}^{b}),$$
(12)

with T_x and T_y being defined as in Eqs. (3) and (9). This model reflects the decomposition of the system's energy due to motion along and perpendicular to the line of centers, regardless of the spheres' orientation with respect to any inertial frame.

If we assume now that the spheres experience a general oscillation in any given direction, they experience an average force depending on the oscillation's alignment with the line of centers. Specifically, the average force along the line of centers will be given by

$$F_x^b = F_x(x_2^b - x_1^b, \dot{x}_1^b, \dot{x}_2^b) + F_y(x_2^b - x_1^b, \dot{y}_1^b, \dot{y}_2^b), \quad (13)$$

where F_x and F_y are defined as in Eqs. (4) and (10). In addition, from the Euler-Lagrange equations for y_i^b there is now a nonzero force that acts on each sphere perpendicular to the line of centers when both x^b and y^b oscillation components are nonzero (previously, we only assumed one or the other, allowing us to ignore this force). The average forces act on the spheres differently and are given by

$$F_{y,1}^{b} = 3\pi \rho \frac{R_1^3 R_2^3}{(x_2^b - x_1^b)^4} [(\dot{x}_2^b - \dot{x}_1^b) \dot{y}_2^b],$$

$$F_{y,2}^{b} = 3\pi \rho \frac{R_1^3 R_2^3}{(x_2^b - x_1^b)^4} [(\dot{x}_2^b - \dot{x}_1^b) \dot{y}_1^b]. \tag{14}$$

Since the only difference in each of the above equations is the last multiplier \dot{y}_i^b , the y^b force of each sphere is effectively determined by the motion of the other.

The last component of our model is to enable actuation, again via internal masses inside each sphere. For this preliminary model, we assume a single mass moving along a fixed

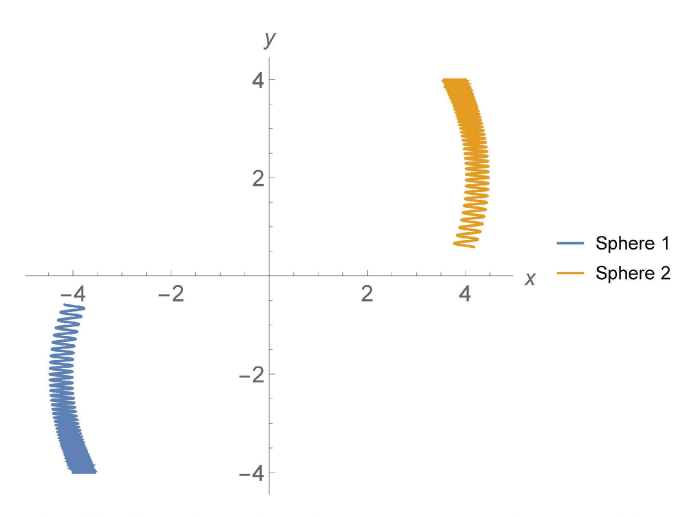


Fig. 10: The trajectories of two spheres, starting at positions (-4,4) and (4,4), due to actuation both along and perpendicular to their moving line of centers.

axis. If this axis is neither aligned with the line of centers nor perpendicular to it, motion along it will contribute both x^b and y^b components of motion to the sphere. We do note that because the components are coupled, richer motion may be achieved adding a second degree of freedom to the mass, a topic of exploration for future work. Here we assume that the mass's single degree of freedom ξ is along the inertial x axis for both spheres, which contributes a kinetic energy

$$T_{\mu}^{b} = \sum_{i=1,2} \frac{1}{2} \mu_{i} \left((\dot{x}_{i}^{b} + \dot{\xi}_{i} \cos \theta)^{2} + (\dot{y}_{i}^{b} - \dot{\xi}_{i} \sin \theta)^{2} \right)$$
 (15)

The total kinetic energy $T^b+T^b_\mu$ thus constitutes the Lagrangian for this planar coupled spheres locomotion problem.

We conclude this section by showing a simple simulation that verifies the predicted behavior of this model. The parameters of the system are set to be those of Section II-B, and the inputs to each of the inertial masses along the inertial x axis are $\xi_1 = \cos(4t)$ and $\xi_2 = -\cos(4t)$. The initial positions of the spheres will be (-4,-4) and (4,4). Because $\theta = \frac{\pi}{4}$, both inputs have equal and out-of-phase contributions in both the x^b and y^b directions. Since $|F_x| > |F_y|$ for the same parameters, the effect of the F_x term will dominate in Eq. (13), resulting in attraction of the spheres along the x^b direction. While this is shown in Fig. 10, we can also observe that the spheres do not move directly toward each other, instead taking a spiral type of trajectory. This is due to nonzero forces on each sphere in the y^b direction, given by Eq. (14). In addition, $F_{y,1}^b$ and $F_{y,2}^b$ act in opposite directions since the inputs are out of phase.

IV. CONCLUSIONS AND FUTURE WORK

In this work we have introduced a novel control problem of using known hydrodynamic interactions between two spherical swimmers to produce desired motion. For both the cases of motion along and motion perpendicular to the line of centers, internal masses are used as an actuation mechanism, and we showed that transfer function analysis can help in choosing the right frequency or phase of input commands for a partially actuated system. Finally, we used our approximations for the aforementioned cases to justify a full model for general planar locomotion.

A more complete characterization of locomotive control in the single degree-of-freedom cases can be aided by an analysis of how the transfer functions depend on parameters such as resonant frequency or initial conditions. It would also be desirable to examine how the choice of input affects behavior such as speed of attraction or repulsion, or transitions from one behavior to another. For the planar case, a formal proof of the negligibility of velocity cross terms in the Lagrangian would make the proposed model more rigorous. Following this, we would like to further explore the implications of having coupled input components in a rotating coordinate frame and how this impacts the choice of control and achievable behavior. Our last simulation also hinted at a rich set of two- and multi-body dynamics that may emerge from these systems.

REFERENCES

- [1] T. Miloh and A. Galper, "Self-propulsion of general deformable shapes in a perfect fluid," *Proceedings of the Royal Society of London A: Mathematical, Physical and Engineering Sciences*, vol. 442, no. 1915, pp. 273–299, 1993.
- [2] T. Chambrion and A. Munnier, "Locomotion and control of a self-propelled shape-changing body in a fluid," *Journal of Nonlinear Science*, vol. 21, no. 3, pp. 325–385, 2011.
- [3] S. D. Kelly, P. Pujari, and H. Xiong, Geometric Mechanics, Dynamics, and Control of Fishlike Swimming in a Planar Ideal Fluid. New York, NY: Springer New York, 2012, pp. 101–116.
- [4] M. Lighthill, "On the squirming motion of nearly spherical deformable bodies through liquids at very small reynolds numbers," *Communica*tions on Pure and Applied Mathematics, vol. 5, no. 2, pp. 109–118, 1952
- [5] B. Felderhof and R. Jones, "Small-amplitude swimming of a sphere," Physica A: Statistical Mechanics and its Applications, vol. 202, no. 1, pp. 119 – 144, 1994.
- [6] A. Shapere and F. Wilczek, "Geometry of self-propulsion at low reynolds number," *Journal of Fluid Mechanics*, vol. 198, pp. 557–585, 04 2006.
- [7] T. Chambrion and A. Munnier, "Generic controllability of 3d swimmers in a perfect fluid," SIAM Journal on Control and Optimization, vol. 50, no. 5, pp. 2814–2835, 2012.
- [8] V. V. Kozlov and D. A. Onishchenko, "Motion of a body with undeformable shell and variable mass geometry in an unbounded perfect fluid," *Journal of Dynamics and Differential Equations*, vol. 15, no. 2-3, pp. 553–570, 2003.
- [9] H. Lamb, *Hydrodynamics*. Cambridge university press, 1932.
- [10] L. M. Milne-Thomson, *Theoretical hydrodynamics*. Courier Corporation, 1968.
- [11] S. Nair and E. Kanso, "Hydrodynamically coupled rigid bodies," *Journal of Fluid Mechanics*, vol. 592, pp. 393–411, 2007.
- [12] E. Kanso and P. K. Newton, "Passive locomotion via normal-mode coupling in a submerged spring-mass system," *Journal of Fluid Mechanics*, vol. 641, pp. 205–215, 2009.
- [13] V. B. Putz and J. M. Yeomans, "Hydrodynamic synchronisation of model microswimmers," *Journal of Statistical Physics*, vol. 137, no. 5-6, p. 1001, 2009.
- [14] R. Golestanian, J. M. Yeomans, and N. Uchida, "Hydrodynamic synchronization at low reynolds number," *Soft Matter*, vol. 7, no. 7, pp. 3074–3082, 2011.
- [15] S. D. Kelly and R. M. Murray, "Geometric phases and robotic locomotion," *Journal of Robotic Systems*, vol. 12, no. 6, pp. 417–431, 1995.
- [16] A. Bloch, P. Krishnaprasad, J. Marsden, and R. Murray, "Nonholonomic mechanical systems with symmetry," Archive for Rational Mechanics and Analysis, vol. 136, no. 1, pp. 21–99, 1996.